A correlation OPTS algorithm for reducing peak to average power ratio of FBMC-OQAM systems[①]

WANG Xing (王　星)[*], MA Tianming[②][*], LI Fengrong[**], ZHAO Qinghua[*]

([*] School of Electrical and Electronic Engineering, Shanghai University of Engineering Science, Shanghai 201620, P. R. China)
([**] Laboratory of Broadband Wireless Technology, Shanghai Institute of Microsystem and Information Technology,
Chinese Academy of Sciences, Shanghai 200050, P. R. China)

Abstract

A correlation overlapping partial transmit sequence (C-OPTS) algorithm is proposed to solve the issue of high complexity of overlapping partial transmit sequence (OPTS) algorithm in suppressing the peak to average power ratio (PAPR) of filter bank multicarrier-offset quadrature amplitude modulation (FBMC-OQAM) signals. The V subblocks in partial transmit sequence (PTS) are regrouped into U combinations according to the correlation coefficient ρ, and overlapping subblocks are allowed between adjacent groups. The search starts from the first group and sets the phase factors of the subsequent groups to 1. When the phase factors of the non-overlapping subblocks in the first group are determined, the subsequent groups are searched in turn to determine their respective phase factors. Starting from the second data block, the data overlapped with it should be taken into account when determining its optimal phase factor vector. Theoretical analysis and simulation results indicate that compared with the OPTS algorithm, the proposed algorithm can significantly reduce the computational complexity at the cost of slight deterioration of PAPR performance. Meanwhile, compared with the even-odd iterative double-layers OPTS (ID-OPTS) algorithm, it can further reduce the complexity and obtain a better PAPR suppression effect.

Key words: filter bank multicarrier (FBMC), offset quadrature amplitude modulation (OQAM), peak to average power ratio (PAPR), overlapping partial transmit sequence (OPTS), correlation coefficient

0　Introduction

Filter bank multicarrier-offset quadrature amplitude modulation (FBMC-OQAM) technology has become one of the candidate physical layer transmission technologies for cognitive radio and the 5G mobile communication[1-2]. Compared with the orthogonal frequency division multiplexing (OFDM) technology, FBMC-OQAM does not need strict orthogonality between each subcarrier, thus, it can not only remove the cyclic prefix to further save the system resources without causing the generation of inter symbol interference (ISI) but also allow some operations such as time-domain synchronization, channel estimation to be carried out separately on each subcarrier, so that the strict restrictions of OFDM in different communication scenarios can be significantly relaxed to better meet the technical re-

quirements in 5G new scene communications[3]. However, FBMC-OQAM still has some defects such as the inability to obtain accurate channel information with conventional schemes and the excessively high peak to average power ratio (PAPR)[4], which hinder its practical application.

This paper mainly studies the problem of high PAPR in FBMC-OQAM. The traditional methods for inhibiting PAPR in OFDM are finite amplitude method[5], compression and expansion method[6], selective mapping (SLM) method[7], partial transmit sequence (PTS) method[8], and so on. Since FBMC-OQAM adopts a non-orthogonal modulation mode, its signal structure is significantly different from that of OFDM. Therefore, employing the PAPR suppression methods of OFDM directly in FBMC-OQAM can not obtain a good restraining effect.

Presently, several methods have been put forward

to mitigate PAPR, which can be divided into three categories.

The first category is the signal distortion method, including chipping method, peak windowing method, and pressure expansion method. A new compression technique based on A-law and μ-law was put forward in Ref. [9]. In Ref. [10], a chipping and iterative compensation method was proposed, which cuts the time domain signal and then applies the iterative Bussgang noise cancellation technique at the receiver to prevent the system performance from deteriorating. Although the above two signal distortion methods can effectively reduce PAPR, they will also incur the out-of-band energy leakage and deteriorate the bit error rate (BER) of the FBMC-OQAM system.

The second category is a non-distortion method, including SLM, PTS and tone reservation (TR). The overlapping PTS (OPTS) method proposed in Ref. [11] considered the time-domain overlap between adjacent data blocks. The optimal phase factor of the current data block was determined by the current data block and its overlapped data blocks. Although the algorithm could effectively reduce PAPR, its complexity increased exponentially with the increase of the number of data blocks. In Ref. [12], an even-odd iterative double-layer OPTS (ID-OPTS) algorithm was proposed, which divides the data block into V subblocks, and then further divides these V subblocks into D sections. Then, the odd-even iteration method was adopted to change the search method of phase factor for the double-layers optimization of the data block, which reduced the computational complexity and achieved a good PAPR suppression effect. Although this kind of non-distortion method will not cause signal distortion, its computational complexity is still high. Therefore, if the non-distortion method can be used to reduce PAPR, how to further reduce its computational complexity should be considered.

The third category is the hybrid method of the above two categories. In Ref. [13], a method combining trellis-based selective mapping (TSLM) and A-law compression was proposed. It applied the TSLM algorithm to obtain the optimal phase rotation sequence and adopts the A-law compression function to further compress high amplitude signal samples and extend the low amplitude signal samples, which not only reduced PAPR effectively but also helped to reduce signal distortion. In Ref. [14], the low complexity dispersion selective mapping and the chipping filtering technique were combined to mitigate PAPR without affecting BER. Although this hybrid method can integrate the advantages of different methods, it still has the demer-

its of high complexity and signals distortion.

To solve the problem of high computational complexity when applying OPTS method to suppress PAPR[11] in the second category, a new suppressing algorithm is proposed, which divides the original V subblocks into U combinations ($U \leq V$), and allows overlapped subblocks between adjacent combinations. Then, a full search on each combination is carried out to determine the phase factor of the non-related subblocks in each combination until all combinations are searched. Theoretical analysis and simulation results indicate that compared with OPTS algorithm[11], the proposed algorithm can significantly reduce the computational complexity at the cost of slight deterioration of PAPR performance, meanwhile, compared with ID-OPTS algorithm[12], it can further reduce the complexity and obtain better PAPR suppression effect.

1 FBMC-OQAM system model

The transmitter model of FBMC-OQAM system is illustrated in Fig. 1. It can be supposed that the mth data symbol input at the transmitter can be expressed as Eq. (1).
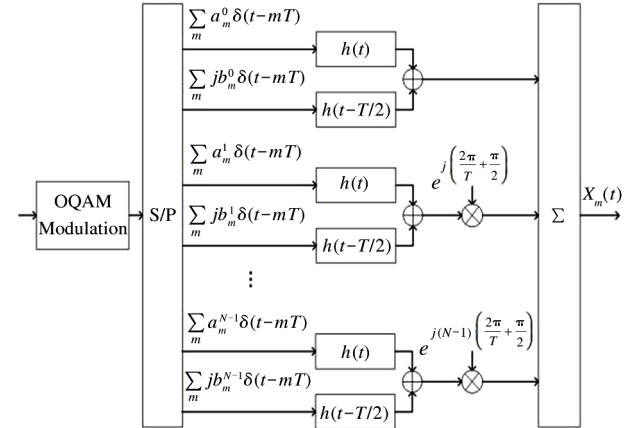

Fig. 1 Block diagram of transmitter structure of FBMC-OQAM system

$$X_m^n = a_m^n + jb_m^n \quad 0 \leq m \leq M-1, \ 0 \leq n \leq N-1 \tag{1}$$

where a_m^n and b_m^n are the real and imaginary parts of the mth data symbol on the nth subcarrier, respectively. N and M are the numbers of all subcarriers and data symbols, respectively. Then, X_m^n is modulated by OQAM to make it interleave $T/2$, where T is the symbol period of FBMC-OQAM. After serial to parallel conversion and filtering by synthetic filter banks, the mth transmission FBMC-OQAM symbol can be obtained by adding all subcarrier signals, which can be expressed by

$$x_m(t) = \sum_{n=0}^{N-1} x_m^n(t)$$

$$= \sum_{n=0}^{N-1} \left[a_m^n h(t - mT) + jb_m^n h\left(t - mT - \frac{T}{2}\right) \right] e^{jn\left(\frac{2\pi}{T}t + \frac{\pi}{2}\right)}$$

$$(2)$$

where $h(t)$ is the impulse response of the prototype filter with KT length and K is the overlapping factor. The prototype filter applied in this paper is European physical layer for dynamic access (PHYDYAS)[15] with $K = 4$, which can be defined as

$$h(t) = 1 + 2\sum_{k=1}^{K-1} H_k \cos\left(2\pi \frac{kt}{KT}\right) \qquad (3)$$

After the sum operation, the final transmission signal $x(t)$ can be described by

$$x(t) = \sum_{m=0}^{M-1} x_m(t) =$$

$$\sum_{m=0}^{M-1}\sum_{n=0}^{N-1} \left[a_m^n h(t - mT) + jb_m^n h\left(t - mT - \frac{T}{2}\right) \right] e^{jn\left(\frac{2\pi}{T}t + \frac{\pi}{2}\right)}$$

$$(4)$$

Owing to the overlapping structure of FBMC-OQAM signal, multiple overlapped data blocks should be considered when reducing PAPR. Thus, the definition of PAPR for FBMC-OQAM system should be redefined. Compared with the definition of PAPR for OFDM system, $x(t)$ can be divided into $M + K$ time intervals by taking time T as an interval (the last interval is $T/2$). Then PAPR of each interval can be defined by[16]

$$PAPR = 10\log_{10} \frac{\max_{iT \leqslant t \leqslant (i+1)T} |x(t)|^2}{E[|x(t)|^2]}$$

$$0 \leqslant i \leqslant M + K - 1 \qquad (5)$$

where $E[|x(t)|^2]$ denotes the expectation of FBMC-OQAM signals.

In this paper, only the absolute value of the amplitude is reduced when reducing PAPR, because the expectation of the input signal can be regarded as a fixed value, and the reduction of the maximum amplitude power is also the reduction of the absolute value of the maximum amplitude.

2   OPTS algorithm

The schematic diagram of the conventional PTS algorithm[8] can be shown in Fig. 2.

The mth data block is divided into V disjoint subblocks, which can be expressed by

$$\boldsymbol{X}_m = [X_m^1, X_m^2, \cdots, X_m^V]^T \quad m = 0,1,\cdots,M-1$$

$$(6)$$

Then, a phase factor vector is generated, which can be given by

$$\boldsymbol{b}_m = \{ b_m^v = e^{j2\pi l/W} \mid l = 0,1,\cdots,W-1 \} \qquad (7)$$

where v ($v = 1, 2, \cdots$), V, and W are the number of allowed phase factors. To reduce the search complexity, the value of the W is 2, and the selection of the phase factor is $+1$ or -1. After multiplying $\boldsymbol{b}_m$ with Eq.(6) and passing through inverse fast Fourier transform (IFFT), the mth transmission signal x_m can be described by

$$x_m = \text{IFFT}\left(\sum_{v=1}^{V} b_m^v X_m^v \right)$$

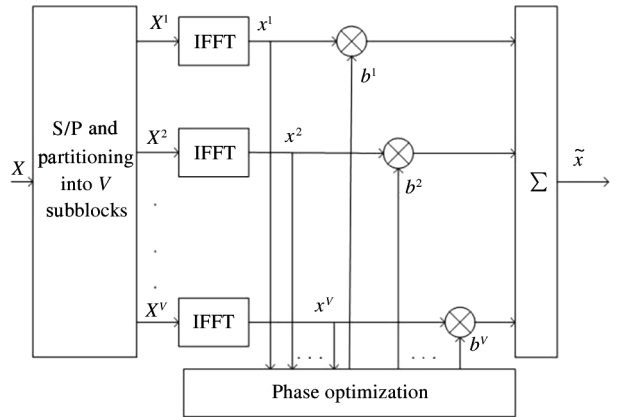$$= \sum_{v=1}^{V} b_m^v \times \text{IFFT}(X_m^v) = \sum_{v=1}^{V} b_m^v x_m^v \qquad (8)$$

Fig. 2   Schematic diagram of conventional PTS algorithm

The purpose of the conventional PTS algorithm is to find out the best phase factor vector $\bar{\boldsymbol{b}}_m$ of each transmission signal, which can be expressed by[17]

$$\bar{\boldsymbol{b}}_m = [\bar{b}_m^1, \bar{b}_m^2, \cdots, \bar{b}_m^V]$$

$$= \arg \min_{b_m^1, b_m^2, \cdots, b_m^V} \max_{(m-1)T \leqslant t \leqslant (m+K-1/2)T} \left| \sum_{v=1}^{V} b_m^v x_m^v \right|$$

$$(9)$$

Thus, the optimal transmission sequence $\tilde{x}_m$ can be described by

$$\tilde{x}_m = \sum_{v=1}^{V} \bar{b}_m^v x_m^v \qquad (10)$$

In FBMC-OQAM system, the overlapping structure of the time-domain between two adjacent data blocks of $x(t)$ can be shown in Fig.3.
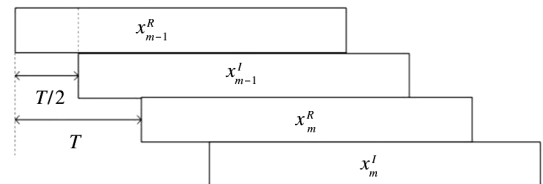

Fig. 3   Time domain structure of adjacent data blocks in FBMC-OQAM system

Since $x(t)$ has the characteristic of time-domain overlapping, thus, applying Eq.(8) directly to miti-

gate PAPR will not obtain a good suppression effect. The OPTS algorithm proposed in Ref. [11] considered the time-domain overlaps between adjacent data blocks. The optimal phase factor of the current data block is determined by the current data block and its overlapped data blocks. Assuming that the optimal phase vectors of the first $M-1$ data blocks are known, the best phase factor vector of the mth block can be expressed by

$$\bar{\boldsymbol{b}}_m = [\bar{b}_m^1, \bar{b}_m^2, \cdots, \bar{b}_m^V] =$$
$$\arg \min_{b_m^1, b_m^2, \cdots, b_m^V (m-1)T \leqslant t \leqslant (m+K-1/2)T} \left| \sum_{n=0}^{m-1} \sum_{v=1}^{V} b_n^v x_{m-1} + \sum_{v=1}^{V} b_m^v x_m^v \right| \tag{11}$$

It is not difficult to find that the overlaps between data blocks in Eq. (11) can be given by

$$x' = \sum_{n=0}^{m-1} \sum_{v=1}^{V} b_n^v x_{m-1} (m-1)T \leqslant m \leqslant \left(m+K-\frac{1}{2}\right)T \tag{12}$$

Then, M optimal phase factor vectors $\bar{\boldsymbol{b}} = [\bar{\boldsymbol{b}}_0, \bar{\boldsymbol{b}}_1, \cdots, \bar{\boldsymbol{b}}_{M-1}]$ can be found and M optimal transmission sequences $\tilde{\boldsymbol{x}} = [\tilde{x}_0, \tilde{x}_1, \cdots, \tilde{x}_{M-1}]$ can be obtained.

Although OPTS algorithm can achieve an ideal PAPR suppression effect, its computational complexity increases exponentially with the increase of sub-blocks[11]. Therefore, in order to apply it to practical communication, it is necessary to further reduce its computational complexity.

3   Correlation OPTS algorithm

In this section, a correlation OPTS (C-OPTS) algorithm is introduced, which recombines the original number of V subblocks into U groups ($U \leqslant V$) to reduce the high complexity of OPTS. Here correlation coefficient ρ is defined as the number of overlapped subblocks in two adjacent groups. Obviously, if there is no overlap, the correlation coefficient $\rho = 0$. Fig. 4 depicts the different grouping situations when the number of subblocks V is 8 and the correlation coefficient ρ is 1, 2, 3, and 5 respectively. According to the inspection, it is not difficult to discover that $\rho + U = V$, $1 \leqslant \rho \leqslant V-1$. If the value of ρ is $V-1$, then the number of combinations U is 1, and there will be no related subblocks among recombination.
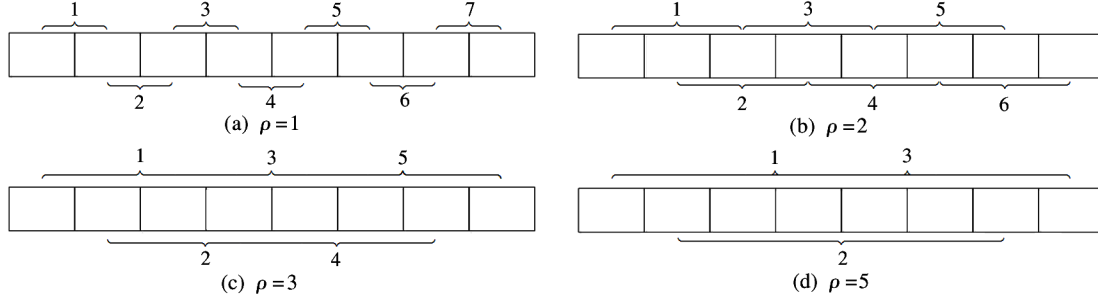

Fig. 4   The recombination of V subblocks ($V=8$) with different values of ρ

Next, a detailed description of the search algorithm in C-OPTS can be described as follows.

Step 1   The V sub-blocks are divided into U groups again, the number of overlapping sub-blocks between adjacent groups is ρ, a full search is performed on the first group, and the phase factors in other combinations are all assigned a value of 1. For example, when $V = 8$, $U = 7$, $\rho = 1$, the full search of the first group can get $2^{\rho+1}$ cases, namely $(1,1)$, $(1,-1)$, $(-1,1)$, and $(-1,-1)$. When the phase factor in other combinations is 1, the following four candidate phase factor vectors $(1,1,1,1,1,1,1,1)$, $(1,-1,1,1,1,1,1,1)$, $(-1,1,1,1,1,1,1,1)$, and $(-1,-1,1,1,1,1,1,1)$ can be obtained.

Step 2   These candidate phase factor vectors are substituted into Eq. (11) for a calculation to obtain the best phase factor vector at this time, and the phase factors of the non-overlapping parts of the first group and the second group are retained. For example, if the vector $(-1, -1, 1, 1, 1, 1, 1, 1)$ is the best phase factor vector, only -1 at the first position is retained.

Step 3   Carrying out a full search for the second group. Except for the reserved phase factors of the first group, the phase factors in other combinations are assigned as 1, and then $(-1, 1, 1, 1, 1, 1, 1, 1)$, $(-1, 1, -1, 1, 1, 1, 1, 1)$, $(-1, -1, 1, 1, 1, 1, 1, 1)$, and $(-1, -1, -1, 1, 1, 1, 1, 1)$ can be obtained. Then repeat step 2 to retain the phase factors of the non-overlapping parts of the second group and the third group.

Step 4   Repeat the above steps until all groups are searched, and the final optimal phase factor vector can be obtained.

Then, the implementation steps of the C-OPTS algorithm with $\rho = 1$ can be described as follows.

Step 1   The register O used to store the over-

lapped part of the data block is set to zero, and the first data block X_1 is divided into V subblocks, which can be described as $X_1 = [X_1^1, X_1^2, \cdots, X_1^V]^T$. Then X_1 is recombined according to Fig. 4(a) to obtain $U = V - 1$ combinations.

Step 2 The phase factor vector is initialized to $b_1 = [1, 1, \cdots, 1]$. The first combination is fully searched, the optimal phase factor $\tilde{b}_1^1$ of the uncorrelated part in the first combination is retained, and the initial phase factor vector is updated to $b_1 = [\tilde{b}_1^1, 1, \cdots, 1]$. Then, the same operation is performed on the second combination, and the initial phase factor vector is updated to $b_1 = [\tilde{b}_1^1, \tilde{b}_1^2, \cdots, 1]$. Thus, the optimal phase factor vector of the first data block can be described as $\tilde{b}_1 = [\tilde{b}_1^1, \tilde{b}_1^2, \cdots, \tilde{b}_1^V]$. At this time, the data that overlaps with the second data block is the data in the interval $[T/2, 4T]$ in the optimized first data block. Since the length of each data block is $4T$, the data in this interval is taken out and 0 is added at the end to make the length be $4T$, and finally saved in register O. Fig. 5 applies the overlapped part of the third data block as an example to describe the data stored in register O, and the overlapped parts of other data blocks can be deduced by analogy.
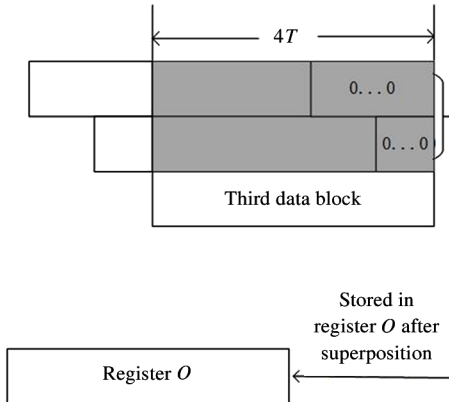

Fig. 5 Schematic diagram of overlapping data stored in register O

Step 3 The second data block is grouped in the same way as the first data block. The optimal phase factor vector of the second data block must satisfy Eq. (11) so that the data stored in the register O and the second data block have the smallest amplitude after being superimposed. In the candidate phase factor vector, the vector meeting the smallest amplitude is saved as $\tilde{b}_2 = [\tilde{b}_2^1, \tilde{b}_2^2, \cdots, \tilde{b}_2^V]$. Finally, the register O is updated according to the method in step 2.

Step 4 Similarly, the optimal phase factor vectors $\tilde{b}_3, \cdots, \tilde{b}_M$ of the remaining $M - 2$ data blocks can also be obtained according to the searching method

mentioned in step 2 and step 3. Accordingly, the M optimal phase factor vectors can be expressed as $\tilde{b} = [\tilde{b}_1, \tilde{b}_2, \cdots, \tilde{b}_M]$.

According to the aforementioned descriptions, the overall flowchart of C-OPTS algorithm can be shown in Fig. 6.
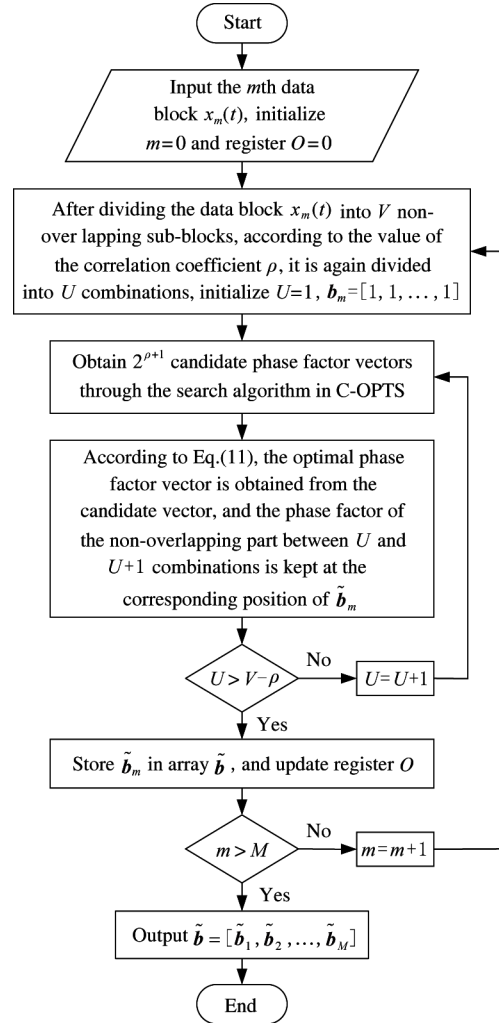

Fig. 6 The flowchart of the C-OPTS algorithm

4   Simulation results and algorithm complexity analysis

4.1   Computational complexity analysis

The following is an analysis of the computational complexity of C-OPTS algorithm. The improvement of algorithm complexity is usually measured by the computational complexity reduction ratio (CCRR), which can be defined by

$$CCRR = \left(1 - \frac{\text{Complexity of new algorithm}}{\text{Complexity of the original lgorithm}}\right) \times 100\%$$

$$(13)$$

From Refs[12], [18] and [19], it is not difficult to find that the real multiplications and real addi-

tions of OPTS algorithm and ID-OPTS algorithm can be given by

$$C_{\text{OPTS}}^{\text{RM}} = 4M\left(L_h + \frac{N}{2}\right)(VN + V2^V) + 2(L_h + 1)MN \tag{14}$$

$$C_{\text{OPTS}}^{\text{RA}} = 2M\left(L_h + \frac{N}{2}\right)\left[(2N - 1)V + (2V - 1)2^V\right] \tag{15}$$

$$C_{\text{ID-OPTS}}^{\text{RM}} = 4M\left(L_h + \frac{N}{2}\right)(VN + V(2V + 2D)) + 2(L_h + 1)MN \tag{16}$$

$$C_{\text{ID-OPTS}}^{\text{AM}} = 2M\left(L_h + \frac{N}{2}\right)\left[(2N - 1)(V + D) + (2V - D)2V + (2D - 1)2D\right] \tag{17}$$

where N, M and V are the numbers of subcarriers, data symbols, and subblocks, respectively. D is the number of outer section optimization in ID-OPTS algorithm, and $L_h = KT$ is the length of the prototype filter.

The difference in computational complexity between C-OPTS algorithm and OPTS algorithm is mainly reflected in the search of their phase factors. Since C-OPTS

algorithm with correlation coefficient ρ can be divided into $V - \rho$ combinations, each combination needs to search phase factor $2^{\rho+1}$ times, therefore, C-OPTS algorithm needs to search $(V - \rho) \times 2^{\rho+1}$ times in total. Therefore, its real multiplications and real additions can be expressed by

$$C_{\text{C-OPTS}}^{\text{RM}} = 4M\left(L_h + \frac{N}{2}\right)\left[VN + (V - \rho)2^{\rho+1}\right] + 2(L_h + 1)MN \tag{18}$$

$$C_{\text{C-OPTS}}^{\text{RA}} = 2M\left(L_h + \frac{N}{2}\right)\left[(2N - 1)V + (2V - 1)2^{\rho+1}\right] \tag{19}$$

Table 1 illustrates the computational complexity and CCRR of the above three algorithms under the conditions of $M = 20$, $N = 64$, $V = 8$, $L_h = 256$, $D = 2$, 4 and $\rho = 1$. According to the inspection, it is not difficult to find that the computational complexity of C-OPTS algorithm is slightly lower than that of ID-OPTS algorithm and significantly lower than that of OPTS algorithm.

Table 1   The computational complexity and CCRR of OPTS, ID-OPTS and C-OPTS

	Computational complexity ($\times 10^7$)				CCRR/%		
	OPTS	ID-OPTS		C-OPTS	Compared with OPTS	Compared with ID-OPTS	
		$D = 4$	$D = 2$	$\rho = 1$		$D = 4$	$D = 2$
Real multiplications	5.9640	1.6878	1.6141	1.3099	78.0	22.4	19.8
Real additions	5.5941	2.0413	2.0275	1.2396	77.8	39.3	38.9

4.2   Performance simulations analysis

The C-OPTS algorithm proposed in the previous section is investigated by the simulation software. Table 2 summarizes the main parameters for the simulations. In order to ensure the reliability of the simulation results, the number of simulation experiments is set to 1000, and ITU-VB[20], which has an obvious relative delay, is applied as the wireless channel model for system simulation.

The performance of PAPR can be measured by the complementary cumulative distribution function (CCDF). It is defined as the probability that PAPR exceeds a given threshold PAPR_0[17], which can be presented as

$$CCDF(N, \text{PAPR}_0) = Pr\{\text{PAPR} > \text{PAPR}_0\}$$
$$= 1 - (1 - e^{-\text{PAPR}_0})^N \tag{20}$$

where N is the number of subcarriers of FBMC-OQAM.

The whole simulation process can be divided into the following three stages.

Firstly, the method of variable control is applied to analyze the influence of parameters ρ, M and modulation modes on the PAPR suppression performance of

the proposed C-OPTS algorithm. The final simulation results can be demonstrated in Fig. 7, from which the following conclusions can be made.

Table 2   System simulation parameters

Parameters	Values/Explanations
Channel bandwidth	8 MHz
Modulation mode	4QAM, 16QAM
Prototype filter	PHYDYAS
Overlapping factor (K)	4
Number of data symbols (M)	30, 200
Number of subcarriers (N)	128
Number of subblocks (V)	8
Number of outer sections (D)	2, 4, 8
Correlation coefficient (ρ)	1, 2, 3, 5
Channel model	ITU-VB
Noise model	Independent identically distributed additive white Gaussian noise (AWGN)

（a）$M = 30$，4QAM

（b）$M = 200$，4QAM

（c）$M = 30$，16QAM
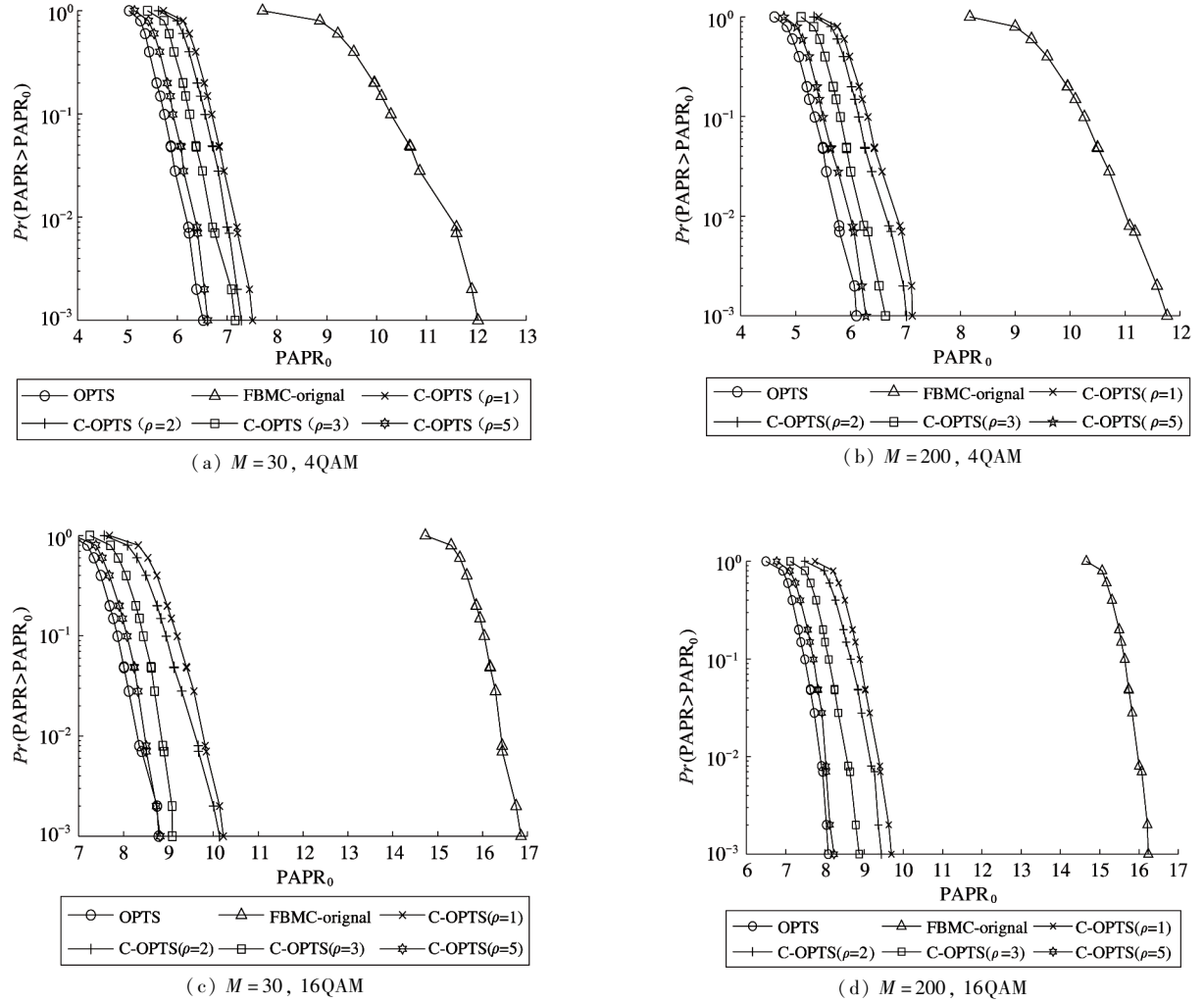

（d）$M = 200$，16QAM

Fig. 7　PAPR performance of C-OPTS algorithm with different parameters and modulation modes

　　（1）The PAPR suppression performance of C-OPTS algorithm at $\rho = 2$，3，5 is 0.16 dB，0.42 dB and 0.89 dB better than that at $\rho = 1$，respectively in Fig. 7（a）. Meanwhile，its PAPR curve at $\rho = 1$ is 0.11 dB，0.49 dB and 0.84 dB lower than that at $\rho = 2$，3，and 5，respectively in Fig. 7（b），which demonstrates that when M is constant，the performance of C-OPTS algorithm to suppress PAPR will be better with the increase of ρ. The main reason is that the number of searched phase factor vectors will increase with the increase of ρ，which increases the possibility of finding a better phase factor vector. While according to Eq. （18）and Eq. （19），it is not difficult to discover that the increase of ρ will also induce a significant increase in computational complexity. Therefore，$\rho = 1$ is more appropriate.

　　（2）Comparing Fig. 7（a）with Fig. 7（b），and Fig. 7（c）with Fig. 7（d），it is easy to find that the difference of M does not affect the effect of C-OPTS algorithm to reduce PAPR. As can be seen from Fig. 4，

no matter what the value of M is，it will be divided into V subblocks for processing. And from Eq. （4），it can be seen that M only affects the length of the transmitted signal $x(t)$，and may reduce the PAPR value of the FBMC-OQAM signal when it is superimposed on each other. As shown in Fig. 7（a）and （b），when $M = 30$ and $M = 200$，the PAPR of the FBMC-OQAM signal itself is 12.11 dB and 11.82 dB，respectively.

　　（3）Comparing Fig. 7（a）with Fig. 7（c），and Fig. 7（b）with Fig. 7（d），it is not difficult to discover that for the same method，the scheme adopting 4QAM modulation will obtain a lower PAPR value than the scheme adopting 16QAM modulation，the main reason lies in the fact that although increasing the modulation order can make the original modulation achieve higher transmission efficiency，unfortunately，it will inevitably increase the probability of high PAPR.

　　Secondly，the performance of PAPR to evaluate C-OPTS with OPTS and ID-OPTS with $V = 8$，$D = 2$，4，$M = 30$ and $\rho = 1$ under different modulation modes

can be shown in Fig. 8. It is not difficult to discover that:

(1) When $\rho = 1$, the PAPR performance of C-OPTS algorithm is 1.11 dB lower than that of OPTS algorithm, which illustrates that C-OPTS algorithm achieves a significant decrease in complexity at the cost of a small deterioration of PAPR performance so that the algorithm can be accepted by the practical systems;

(2) The PAPR performance of C-OPTS is 0.38 dB and 1.27 dB better than that of ID-OPTS algorithm when $D = 4$ and $D = 2$, respectively, which is due to the fact that the phase factor vectors that can be searched by the even-odd iteration method in ID-OPTS algorithm

are fixed and repeated. Taking $V = 4$ and $D = 2$ as examples, 64 possible phase factor vectors can be searched according to ID-OPTS algorithm. Unfortunately, only 16 of them are effective phase factor vectors, and the remaining 48 are the repetition of these 16 phase factor vectors, which inevitably leads to high computational complexity and poor PAPR mitigation. While C-OPTS algorithm proposed in this paper applies full search in each combination, which can further improve the randomness of the phase factor vector searched, so it can search for a better phase factor vector.
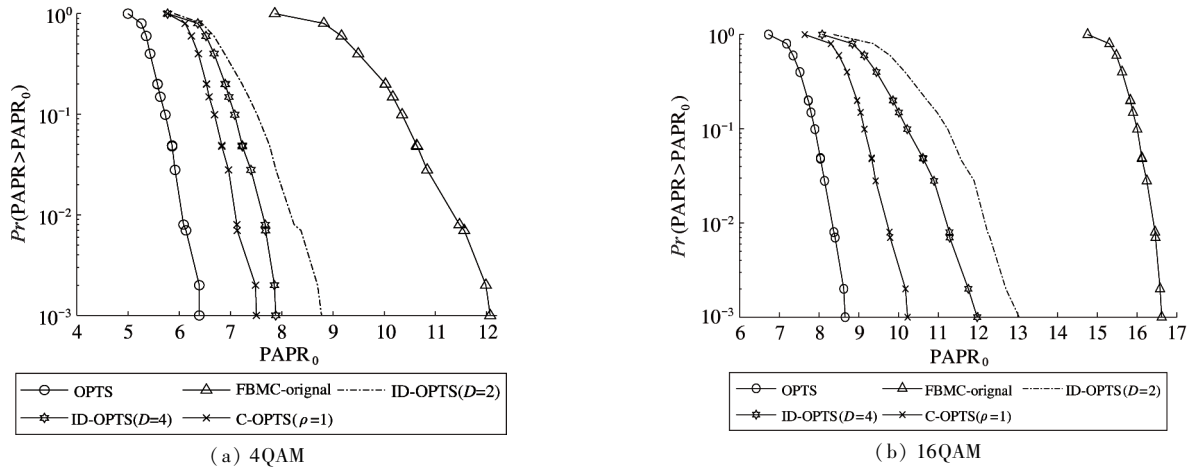

(a) 4QAM   (b) 16QAM

Fig. 8 Comparison of PAPR performance of various algorithms with $V = 8$, $D = 2, 4$, $M = 30$ and $\rho = 1$

Finally, the simulations to evaluate the BER performances of the above algorithms with the same parameters and modulation modes can be shown in Fig. 9. The simulation results are demonstrated in Fig. 9, from which the following conclusions can be made.

(1) The BER performance of the system with C-OPTS algorithm is obviously better than that with ID-

OPTS algorithm and is very close to that with OPTS algorithm under the same promise of the same modulation mode. The main reason is that the correlation scheme introduced in C-OPTS is essentially a non-distortion technology, which will not deteriorate the BER performance of the system. In the meantime, the introduction of a correlation scheme expands the search range
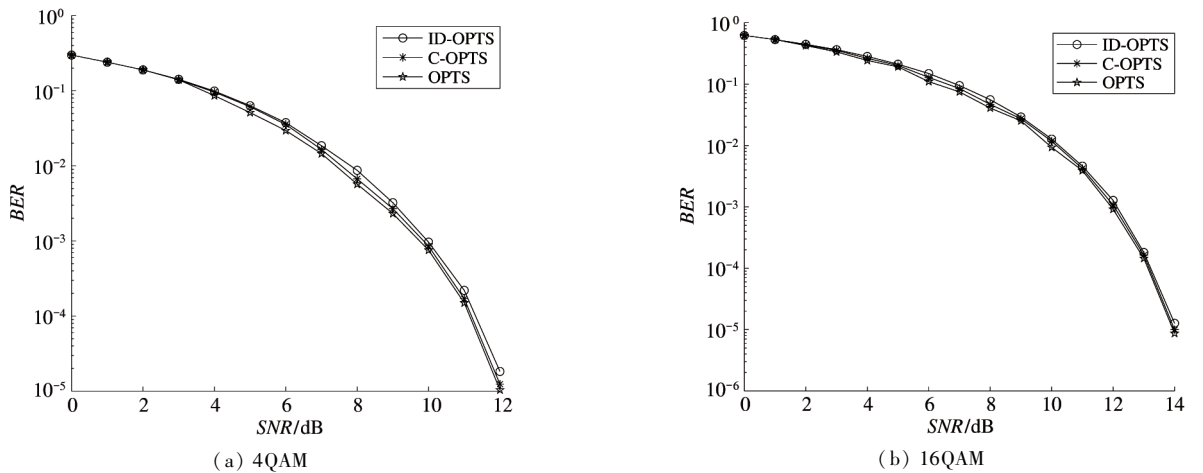

(a) 4QAM   (b) 16QAM

Fig. 9 Comparison of BER performance of various algorithms with $V = 8$, $D = 4$, $M = 30$ and $\rho = 1$

of the phase factor and then the peak probability of the signal can be further reduced, which will undoubtedly raise the BER performance of the system;

(2) For the same scheme, applying 4QAM modulation can achieve better BER performance than that applying 16QAM modulation. For instance, the SNR of C-OPTS is raised by approximately 2 dB when the BER performance is 10^{-5}. The primary reason is that 4QAM has a larger minimum Euclidean distance than 16QAM, that is to say, when the received signals with 4QAM are demodulated, the anti-interference performance will become better, therefore, the system performance can be further improved accordingly.

5   Conclusions

In this paper, C-OPTS algorithm is presented, which reduces the computational complexity by grouping V subblocks for a local solution, and adds correlation coefficients in the search process to limit the global complexity. Theoretical analysis and simulation results indicate that compared with OPTS algorithm, the proposed algorithm can significantly reduce the computational complexity at the cost of slight deterioration of PAPR performance, meanwhile, compared with the even-odd ID-OPTS algorithm, it can further reduce the complexity and obtain better PAPR suppression effect and structure, which is promising for practical applications.

References

[1] CHOI K. Alamouti coding for DFT spreading-based low PAPR FBMC[J]. *IEEE Transactions on Wireless Communications*, 2019, 18(2):926-941

[2] CAI Y, QIN Z, CUI F, et al. Modulation and multiple access for 5G networks[J]. *IEEE Communications Surveys and Tutorials*, 2018, 20(1):629-646

[3] CHOI K. Inter-user frequency offset resilient uplink FBMC by DFT spreading and cyclic shift[J]. *IEEE Wireless Communications Letters*, 2019, 8(3):925-928

[4] NA D, CHOI K. Generalization of the phase shift condition in "Intrinsic ICI-Free Alamouti Coded FBMC"[J]. *IEEE Communications Letters*, 2017, 21(8):1747-1750

[5] TANG B, QIN K, ZHANG X, et al. A clipping-noise compression method to reduce PAPR of OFDM signals [J]. *IEEE Communications Letters*, 2019, 23(8):1389-1392

[6] ZHANG T, ZOU Y, SUN J, et al. Improved companding transform for PAPR reduction in ACO-OFDM-based VLC systems[J]. *IEEE Communications Letters*, 2018, 22(6):1180-1183

[7] GOPI S, KALYANI S. An optimized SLM for PAPR reduction in non-coherent OFDM-IM[J]. *IEEE Wireless Communications Letters*, 2020, 9(7):967-971

[8] CHEN H, CHUNG K. A low complexity PTS technique using minimal trellis in OFDM systems[J]. *IEEE Transactions on Vehicular Technology*, 2018, 67(1):817-821

[9] HASAN A, ZEESHAN M, MUMTAZ M A, et al. PAPR reduction of FBMC-OQAM using A-law and Mu-law companding[C]//Proceedings of the 12th International Conference ELEKTRO 2018, Mikulov, Czekh, 2018:1-4

[10] KOLLAR Z, HORVATH P. PAPR reduction of FBMC by clipping and its iterative compensation[J]. *Journal of Computer Networks and Communications*, 2012(1):1-11

[11] SHI N, WEI S. A partial transmit sequences based approach for the reduction of peak-to-average power ratio in FBMC system[C]//Proceedings of the 25th Wireless and Optical Communication Conference, Chengdu, China, 2016:1-3

[12] LI R, TANG Q. Research on the algorithm for reducing PAPR of FBMC-OQAM[J]. *Journal of Chongqing University of Posts and Telecommunications (Natural Science Edition)*, 2017, 29(5):625-632 (In Chinese)

[13] LI X, WANG D, LI Z, et al. A hybrid TSLM and A-law companding scheme for PAPR reduction in FBMC-OQAM systems[C]//Proceedings of the International Wireless Communications and Mobile Computing, Limassol, Cyprus, 2020:1077-1081

[14] YI X, WANG B, ZHAO W, et al. Hybrid PAPR reduction algorithm using low complexity dispersive selective mapping with clipping and filtering for FBMC/OQAM[C] //Proceedings of the 11th International Conference on Ubiquitous and Future Networks, Zagreb, Croatia, 2019: 532-537

[15] LV S, ZHAO J, YANG L, et al. Genetic algorithm based bilayer PTS scheme for peak-to-average power ratio reduction of FBMC/OQAM signal[J]. *IEEE Access*, 2020, 8:17945-17955

[16] WANG H, WANG X, XU L, et al. Hybrid PAPR reduction scheme for FBMC/OQAM systems based on multi data block PTS and TR methods[J]. *IEEE Access*, 2016, 4:4761-4768

[17] CHENG X, LIU D, SHI W, et al. A novel conversion vector-based low-complexity SLM scheme for PAPR reduction in FBMC/OQAM systems[J]. *IEEE Transactions on Broadcasting*, 2020, 66(3):656-666

[18] YE C, LI Z, JIANG T, et al. PAPR reduction of OQAM-OFDM signals using segmental PTS scheme with low complexity[J]. *IEEE Transactions on Broadcasting*, 2014, 60(1):141-147

[19] HE Z, ZHOU L, CHEN Y, et al. Low-complexity PTS scheme for PAPR reduction in FBMC-OQAM systems [J]. *IEEE Communications Letters*, 2018, 22(11): 2322-2325

[20] RECOMMENDATION. ITU-R M.1225. Guidelines for evaluation of radio transmission technologies for IMT-2000 [S]. Geneva, Switzerland: International Telecommunication Union, 1997

WANG Xing, born in 1995. She is an M. S. candidate at Shanghai University of Engineering Science. She received her B. S. degree from Huaiyin Normal University in 2017. Her research interests include FBMC communication technology and PAPR reduction technology.